The influence of stimulated temperature-dependent emission cross section on intracavity optical parametric oscillator

S Samimi and A Keshavarz†

Department of Physics, Shiraz University of Technology, Shiraz, Iran

(Received 2 August 2016; revised manuscript received 18 October 2016; published online 10 January 2017)

In this paper, the influence of temperature on the intracavity optical parametric oscillator (IOPO) is investigated by using the stimulated temperature-dependent emission cross section of laser crystal. The rate equations under plane wave approximation have been used for simulation of signal output pulse. Results show that the signal output pulse width is decreased by increasing the laser crystal temperature. Also, the signal output energy is increased by the increasing of the laser crystal temperature. The simulation results for IOPO based on Nd:YAG and Nd:YVO_4, show that the signal pulse energies are increased by 3.2 and 5.6 times respectively when the laser crystal temperature increased from 15 °C to 300 °C. The presented model indicates that the temperature sensitivity of Nd:YVO_4-based IOPOs is more than that of Nd:YAG-based IOPOs which is expected from a physical point of view.

Keywords: nonlinear optic, two-wave mixing, parametric oscillators and amplifiers

PACS: 42.65.Yj, 42.55.Xi **DOI:** 10.1088/1674-1056/26/2/024207

1. Introduction

The coherent electromagnetic wave in near to mid-infrared (IR) spectrum has wide applications in industry, environmental monitoring, spectroscopy, telecommunication,[1–3] and so on. The intracavity optical parametric oscillators provide a practical devise to obtain the coherent electromagnetic wave in this spectrum.[4–6] The operation of the IOPO is based on second nonlinear susceptibility due to two-wave mixing.[7] Also the intracavity optical parametric oscillators can provide practical devices to generate femtosecond pulses which are tunable in the near to mid-IR band.[8,9] A tunable cascaded optical parametric oscillator is presented in Ref. [10] by using chirp-assisted aperiodically poled lithium niobate as nonlinear crystal in which the temperature tuning used to satisfy the phase-matching condition.

A successful theoretical model which describes the dynamics of IOPOs characteristic in the pulse regime, was introduced in 1996 by Debuisschert.[11] This model is known as rate equations model because of solving rate equations for a practical device. The results provided by this model has been used to study the practical setup. In the previous experimental researches, the IOPOs have been studied experimentally in which the experimental data were in good agreement with results of this model.[12–16] The rate equations model has been used to optimize the output coupler of the IOPO.[17]

Influence of energy transfer upconversion (ETU) has been investigated by using rate equations with top-hat beam spatial distribution.[18] The ETU effect causes the beam size to have a value in which the maximum average signal output power can be obtained.

As the thermal loss becomes comparable with intrinsic loss of the cavity in the high power IOPO, the influence of thermal-induced diffraction loss on the IOPO has been studied by using rate equation with Gaussian beam profile of TEM_{00}.[19]

The stimulated emission cross section of laser crystal is a critical factor in the IOPO. This factor can be depended on the crystal boundary temperature. The stimulated temperature-dependent emission cross section has been presented in Ref. [20]. This model was used for practical setup of solid state laser in which the theoretical results were in good agreement with the experimental data.[21] Therefore, the usage of the stimulated temperature-dependent emission cross section with rate equations model has provided a successful model to describe solid state lasers.

In this paper, the normalized rate equations has been obtained for the IOPO. In the rate equations, the stimulated emission cross section is substituted by the stimulated temperature-dependent emission cross section introduced in Ref. [20]. The obtained rate equations are solved numerically. The signal output pulse characteristic is investigated by using the numerical solution of the rate equations.

2. Theoretical model

Theoretical model for setup as shown in Fig. 1 has been presented. According to Fig. 1 the laser beam is oscillated in the fundamental cavity which is created by mirrors RM and OC. Therefore, the mirrors RM and OC have high reflectivity at the laser wavelength. The signal beam is resonated in the OPO cavity, which is surrounded between mirrors M_1 and

†Corresponding author. E-mail: Keshavarz@sutech.ac.ir

© 2017 Chinese Physical Society and IOP Publishing Ltd

OC. Therefore, M_1 has high reflectivity at the signal wavelength. As a part of signal energy should exit from the OPO cavity as output, the OC has partial reflectivity at the signal wavelength. The idler beam does not experience resonance because single resonator IOPO is considered in this paper.

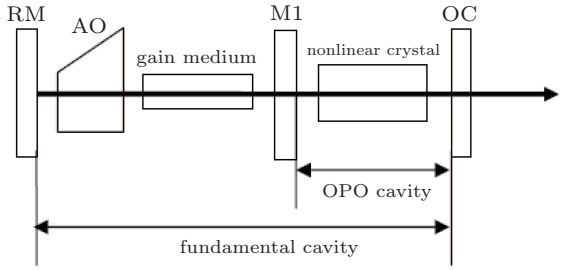


Fig. 1. The schematic diagram of an intracavity optical parametric oscillator.[11–14]

The rate equations under plane-wave approximation for the setup shown in Fig. 1 are given by[11]

$$\frac{\mathrm{d}n(t)}{\mathrm{d}t} = -\gamma c\sigma(T)\phi_{\mathrm{l}}(t)n(t), \tag{1}$$

$$\frac{\mathrm{d}\phi_{\mathrm{l}}(t)}{\mathrm{d}t} = c\sigma(T)\frac{l_{\mathrm{lc}}}{l_{\mathrm{f}}}\phi_{\mathrm{l}}(t)n(t) - c\sigma_{\mathrm{nl}}\frac{l_{\mathrm{nl}}}{l_{\mathrm{f}}}\phi_{\mathrm{l}}(t)\phi_{\mathrm{s}}(t) - \frac{\phi_{\mathrm{l}}(t)}{\tau_{\mathrm{l}}}, \tag{2}$$

$$\frac{\mathrm{d}\phi_{\mathrm{s}}(t)}{\mathrm{d}t} = c\sigma_{\mathrm{nl}}\frac{l_{\mathrm{nl}}}{l_{\mathrm{OPO}}}\phi_{\mathrm{l}}(t)\phi_{\mathrm{s}}(t) - \frac{\phi_{\mathrm{s}}(t)}{\tau_{\mathrm{s}}}, \tag{3}$$

where $n(t)$, $\phi_{\mathrm{l}}(t)$, and $\phi_{\mathrm{s}}(t)$ are the population inversion, laser, and signal photon densities respectively; γ and c are the inversion reduction factor of laser crystal and light speed in the vacuum respectively; l_{lc} and l_{nl} are the laser and nonlinear crystal lengths respectively; l_{f} and l_{OPO} are the fundamental and OPO resonators lengths.

The τ_{l} and τ_{s} are the fundamental and OPO resonators photon lifetimes given by the following equation

$$\tau_j = \frac{t_{\mathrm{r}j}}{L_j + \ln(1/R_j)} \quad \text{with } j = \mathrm{l}, \mathrm{s}, \tag{4}$$

where t_{rl} and t_{rs} are the round trip time of fundamental and OPO resonators; L_{l} and L_{s} are the fundamental and OPO resonators intrinsic losses respectively; Also R_{l} and R_{s} are the output coupler reflectivity at laser and signal wavelength respectively. σ_{nl} is the nonlinear process cross section and is given by[22]

$$\sigma_{\mathrm{nl}} = \frac{\hbar\omega_{\mathrm{l}}\omega_{\mathrm{s}}\omega_{\mathrm{id}}d_{\mathrm{eff}}^2 l_{\mathrm{nl}}}{\varepsilon_0 c^2 n_{\mathrm{l}}^2 n_{\mathrm{s}}^2 n_{\mathrm{id}}}\left(1 - \frac{\alpha_{\mathrm{id}}l_{\mathrm{nl}}}{3}\right), \tag{5}$$

where $\hbar = h/2\pi$ with h being planck constant, ω_{l}, ω_{s}, and ω_{id} are the circular frequency of fundamental, signal, and idler photons, d_{eff} is the effective nonlinear coefficient, l_{nl} is nonlinear crystal length, α_{id} is the absorption coefficient at idler wavelength, ε_0 is the dielectric constant of the vacuum, n_{l}, n_{s}, and n_{id} are the average refractive index at fundamental, signal, and idler wavelength respectively. The stimulated temperature-dependent emission cross section, $\sigma(T)$, is given by[20]

$$\sigma(T) = \sigma_0\left(e_0 - e_1 T + e_2 T^2 - e_3 T^3\right), \tag{6}$$

where σ_0 is the stimulated emission cross section in the standard temperature and e_i is the i-th term coefficient in the Taylor expansion which depends on the laser crystal material. The e_i for Nd:YAG and Nd:YVO_4 are presented in Table 1.

Table 1. The term coefficient e_i for Nd:YAG and Nd:YVO_4 at $T_0 = 20\,^{\circ}\mathrm{C}$.[20]

Laser crystal	e_0	$e_1/10^{-3}\ \mathrm{K}^{-1}$	$e_2/10^{-6}\ \mathrm{K}^{-1}$	$e_3/10^{-9}\ \mathrm{K}^{-1}$
Nd:YAG	1.062	2.723	2.538	0.5267
Nd:YVO_4	1.120	6.241	17.10	18.47

The threshold value of inversion population for laser photons generation can be obtained by setting

$$\frac{\mathrm{d}\phi_{\mathrm{l}}(t)}{\mathrm{d}t} = \phi_{\mathrm{s}}(t) = 0$$

in Eq. (2)

$$n_{\mathrm{th}} = \frac{L_{\mathrm{l}} + \ln(1/R_{\mathrm{l}})}{2\sigma(T)l_{\mathrm{lc}}} \tag{7}$$

by defining normalized values as follows:

$$N(t) = \frac{n(t)}{n_{\mathrm{th}}}, \tag{8}$$

$$\Phi_j(t) = \frac{2\gamma\sigma(T)l_{\mathrm{f}}}{L_{\mathrm{l}} + \ln(1/R_{\mathrm{l}})}\phi_j(t) \quad \text{with } j = \mathrm{l}, \mathrm{s}, \tag{9}$$

$$\tau = \frac{t}{\tau_{\mathrm{l}}}. \tag{10}$$

The normalized rate equation can be obtained as

$$\frac{\mathrm{d}N(\tau)}{\mathrm{d}\tau} = -N(\tau)\Phi_{\mathrm{l}}(\tau), \tag{11}$$

$$\frac{\mathrm{d}\Phi_{\mathrm{l}}(\tau)}{\mathrm{d}\tau} = N(\tau)\Phi_{\mathrm{l}}(\tau) - M_{\mathrm{s}}\Phi_{\mathrm{l}}(\tau)\Phi_{\mathrm{s}}(\tau) - \Phi_{\mathrm{l}}(\tau), \tag{12}$$

$$\frac{\mathrm{d}\Phi_{\mathrm{s}}(\tau)}{\mathrm{d}\tau} = G\Phi_{\mathrm{l}}(\tau)\Phi_{\mathrm{s}}(\tau) - K\Phi_{\mathrm{s}}(\tau), \tag{13}$$

where M_{s}, G, and K are given below

$$M_{\mathrm{s}} = \frac{\sigma_{\mathrm{nl}}l_{\mathrm{nl}}}{\gamma\sigma(T)l_{\mathrm{f}}},$$

$$G = M_{\mathrm{s}}\frac{l_{\mathrm{f}}}{l_{\mathrm{OPO}}},$$

$$K = \frac{L_{\mathrm{s}} + \ln(1/R_{\mathrm{s}})}{L_{\mathrm{l}} + \ln(1/R_{\mathrm{l}})}.$$

Equations (11)–(13) are the normalized rate equations under plane-wave approximation. The pulse energy can be calculated by the solution of the normalized rate equations. The pulse energy is given by[23]

$$E_{\mathrm{s}} = \frac{\pi w_{\mathrm{s}}^2\hbar\omega_{\mathrm{s}}}{4\gamma\sigma(T)}\ln\left(\frac{1}{R_{\mathrm{s}}}\right)\int_0^{\infty}\Phi_{\mathrm{s}}(\tau)\,\mathrm{d}\tau, \tag{14}$$

where w_s is the beam radii of signal pulse. By substituting Eq. (6) into Eq. (14), we obtain

$$E_s = \frac{\pi w_s^2 \hbar \omega_s}{4\gamma\sigma_0} \ln\left(\frac{1}{R_s}\right) \frac{\int_0^\infty \Phi_s(\tau)\,\mathrm{d}\tau}{e_0 - e_1 T + e_2 T^2 - e_3 T^3}. \quad (15)$$

According to Eq. (15) for a specified setup, the important temperature-dependent factor in the signal pulse energy is

$$F(T) = \frac{\int_0^\infty \Phi_s(\tau)\,\mathrm{d}\tau}{e_0 - e_1 T + e_2 T^2 - e_3 T^3}. \quad (16)$$

This factor plays important role in the signal pulse characteristic which will be discussed in the next section.

3. Numerical analysis

In this section the pulse parameter and signal output characteristic is presented according to the solution of the rate equations given by Eqs. (11)–(13).

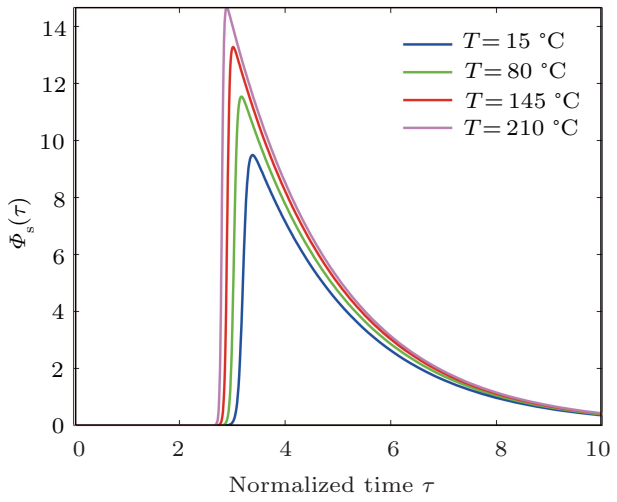


Fig. 2. (color online) The signal pulse shape at various temperatures for Nd:YAG.

For Nd:YAG and Nd:YVO_4, the validity ranges of Eq. (6) are 15 °C–600 °C and 15 °C–350 °C respectively.[20] As practical examples, the signal pulse shapes are plotted in Figs. 2 and 3 for Nd:YAG and Nd:YVO_4. The data detailed in Table 2 are used to plot these figures.

Table 2. Data used to solve normalized rate equations.

Normalized initial inversion population $N(0)$	M_s	G	K
12	2	4	0.5

Figures 2 and 3 show that the peak of the signal pulse is increased by increasing the laser crystal temperature. For Nd:YAG and Nd:YVO_4, as laser crystal temperature increased from 15 °C to 210 °C the peak pulse increased by 1.55 and 1.7 times respectively. Also the signal pulses generate faster as the laser crystal temperature increased.

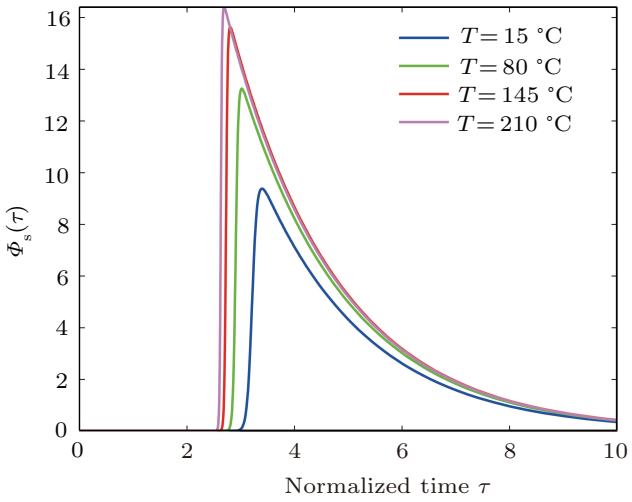


Fig. 3. (color online) The signal pulse shape at various temperatures for Nd:YVO_4.

As stated at the end of the previous section the temperature-dependent factor $F(T)$ plays important roles in the signal pulse characteristic. Therefore the factor $F(T)$ is shown as a function of laser crystal temperature for Nd:YAG and Nd:YVO_4 in Figs. 4 and 5 respectively.

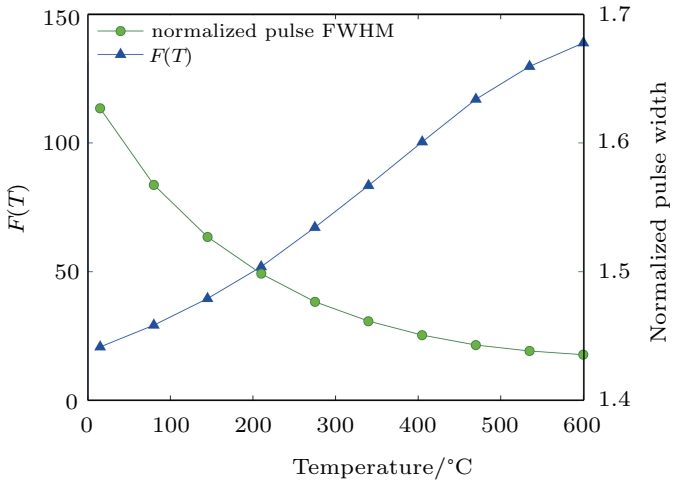


Fig. 4. (color online) $F(T)$ factor and normalized pulse full width at half maximum (FWHM) as a function of temperature for Nd:YAG.

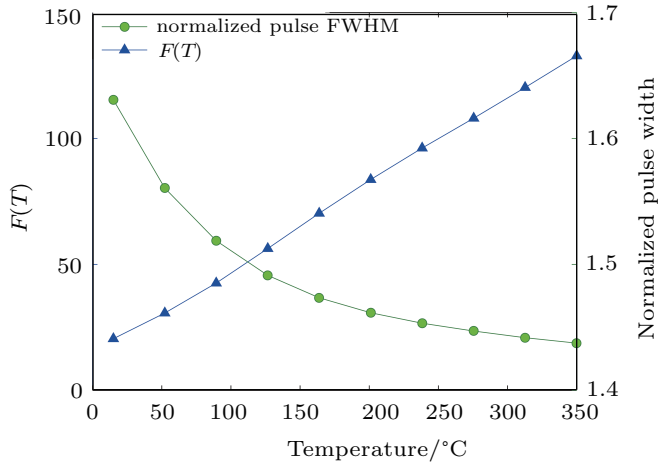


Fig. 5. (color online) $F(T)$ factor and normalized pulse FWHM as a function of temperature for Nd:YVO_4.

From the Figs. 4 and 5 it is seen that the factor $F(T)$ increases as the laser crystal temperature increases. Therefore the pulse energy increases with the increase of the laser crystal temperature, because the signal pulse energy is proportional to the factor $F(T)$. Figure 4 shows that for Nd:YAG the factor $F(T)$ is increased by 3.2 times as temperature is increased from 15 °C to 300 °C. Also Figure 5 shows that the factor $F(T)$ for Nd:YVO_4 is increased by 5.6 times as temperature increased from 15 °C to 300 °C. Therefore the temperature sensitivity of Nd:YVO_4 is more than Nd:YAG.

The normalized pulse widths (FWHM) are plotted as a function of the laser crystal temperature for Nd:YAG and Nd:YVO_4 in Figs. 4 and 5 respectively. From Figs. 4 and 5 it can be concluded that the normalized pulse widths are decreased as the laser crystal temperature increases. For Nd:YAG and Nd:YVO_4 as the temperature varied from 15 °C to 300 °C the normalized pulse widths decreased 9% and 12% respectively.

The physical reason for this signal pulse behavior with respect to temperature is that, the maximum value of Φ_l is increased as rise of the laser crystal temperature and so the factor $F(T)$, which can result to generate narrower signal pulse with more pick pulse energy because the signal output energy is proportional to the factor $F(T)$.

4. Conclusion

In this paper the temperature-dependent signal pulse characteristic of IOPO has been investigated by developing actively Q-switched rate equations using the stimulated temperature-dependent emission cross section. As the laser crystal temperature increases the normalized peak of the signal pulse also increases and the signal pulse generates faster. For Nd:YAG- and Nd:YVO_4-based IOPO, the peak of the normalized signal pulse is increased by 1.55 and 1.7 times respectively as the laser crystal temperature varied from 15 °C to 210 °C.

The signal pulse energy increases as the laser crystal temperature increases. The simulation results for IOPO based on Nd:YAG and Nd:YVO_4 show that the signal pulse energies are increased by 3.2 and 5.6 times respectively when the laser crystal temperature increases from 15 °C to 300 °C. Also the signal pulse width is decreased by increasing the laser crystal temperature. For Nd:YAG- and Nd:YVO_4-based IOPO, the signal pulse widths decreased to 9% and 12% respectively as the laser crystals temperature varied from 15 °C to 300 °C. The presented model shows that the temperature sensitivity of Nd:YVO_4-based IOPOs is more than that of the Nd:YAG-based IOPOs which is expected from a physical point of view. The developed rate equations presented in this paper can be used to design temperature-sensitive IOPO systems.

References

[1] Ding X, Sheng Q, Chen N, Yu X Y, Wang R, Zhang H, Wen W Q, Wang P and Yao J Q 2009 *Chin. Phys. B* **18** 4314
[2] Liu J L, Liu Q, Li H, Li P and Zhang K S 2011 *Chin. Phys. B* **20** 114215
[3] Wan Y, Zeng Q Y, Zhu D Y, Han K, Li T, Han H, Yu S F and Su X Z 2004 *Chin. Phys.* **13** 1402
[4] Liu S D, Wang Z W, Zhang B T, He J L, Hou J, Yang K J, Wang R H and Liu X M 2014 *Chin. Phys. Lett.* **31** 024204
[5] Zheng X H, Zhang B F, Jiao Z X and Wang B 2016 *Chin. Phys. B* **25** 014208
[6] Han K Z, Ning J, He J L, Hou J, Zhang B T and Wang Z W 2015 *Chin. Phys. Lett.* **32** 054203
[7] Boyd R W 2003 *Nonlinear Optics* (New York: Academic Press)
[8] Shen Z W, Wang Z H, Zhang W, Fan H T, Teng H and Wei Z Y 2014 *Chin. Phys. Lett.* **31** 014207
[9] Tian W L, Wang Z H, Zhu J F and Wei Z Y 2016 *Chin. Phys. B* **25** 014207
[10] Chen T, Shu R, Ge Y and Chen Z 2016 *Chin. Phys. B* **25** 014209
[11] Debuisschert T, Raffy J, Pocholle J P and Papuchon M 1996 *J. Opt. Soc. Am. B* **13** 1569
[12] Bai F, Wang Q, Liu Z, Zhang X, Wan X, Lan W, Jin G, Tao X and Sun Y 2012 *Opt. Express* **20** 807
[13] Huang Y, Huang Y, Cho C and Chen Y 2013 *Opt. Express* **21** 7583
[14] Huang H, He J, Dong X, Zuo C, Zhang B, Qiu G and Liu Z 2008 *Appl. Phys. B* **90** 43
[15] Dabu R, Fenic C and Stratan A 2001 *Appl. Opt.* **40** 4334
[16] Bai F, Wang Q, Liu Z, Zhang X, Wan X, Lan W, Jin G and Zhang H 2012 *IEEE J. Quantum Electron.* **48** 581
[17] Chen Y, Chen S, Tsai S and Lan Y 2003 *Appl. Phys. B* **77** 505
[18] Keshavarz A and Samimi S 2015 *Laser Phys.* **25** 095401
[19] Samimi S and Keshavarz A 2016 *Opt. Commun.* **359** 184
[20] Sato Y and Taira T 2012 *Opt. Mater. Express* **2** 1076
[21] Nie M, Liu Q, Ji E and Gong M 2015 *Appl. Opt.* **54** 8383
[22] Liu Z, Wang Q, Zhang X, Chang J, Wang H, Fan S, Sun W, Jin G, Tao X, Zhang S, *et al*. 2008 *Appl. Phys. B* **92** 371
[23] Zhang X, Zhao S, Wang Q, Ozygus B and Weber H 1999 *IEEE J. Quantum Electron.* **35** 1912